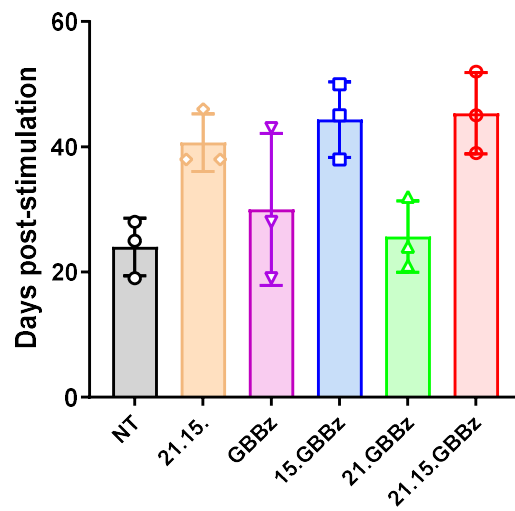
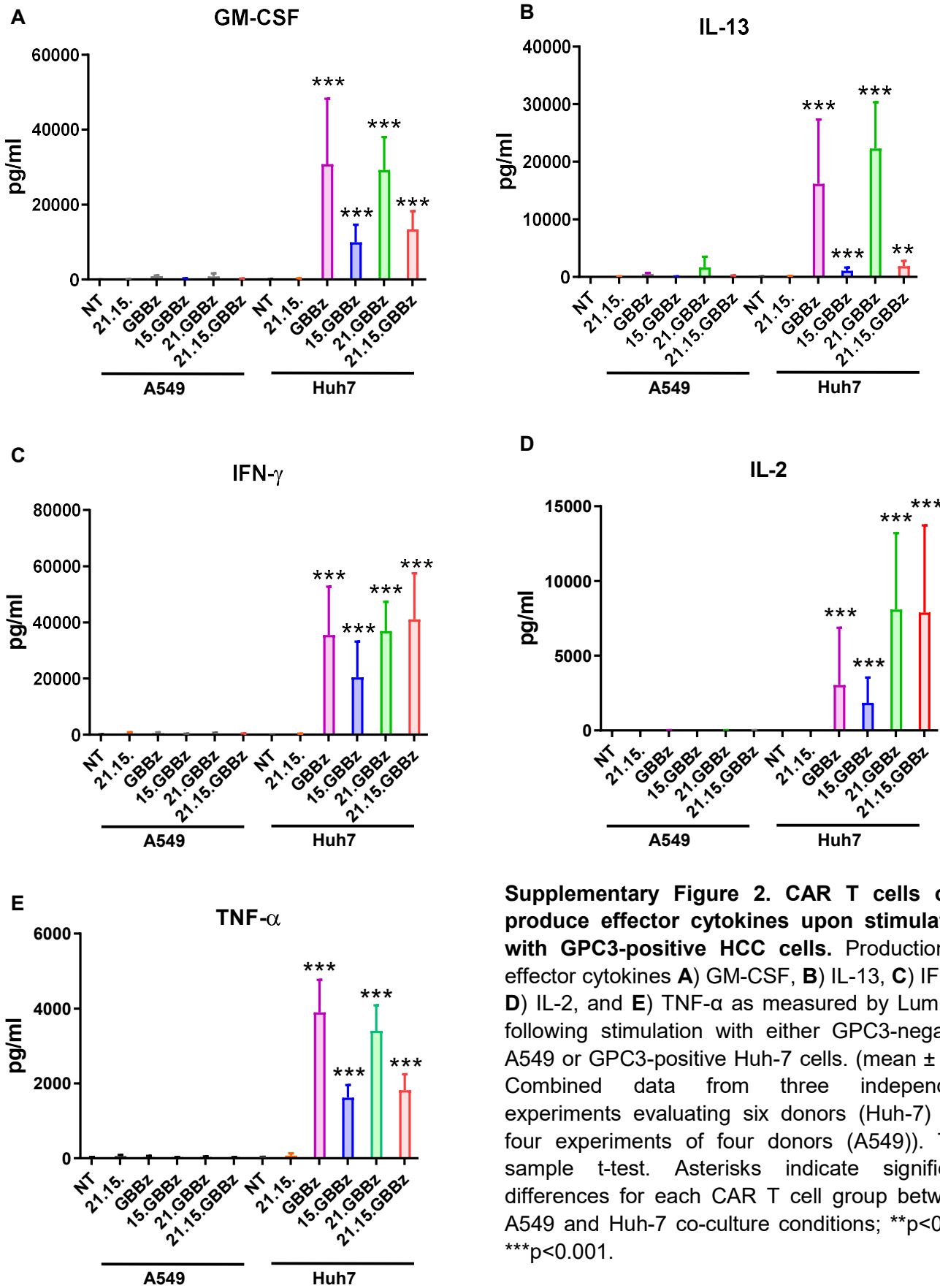


Supp Fig. 1



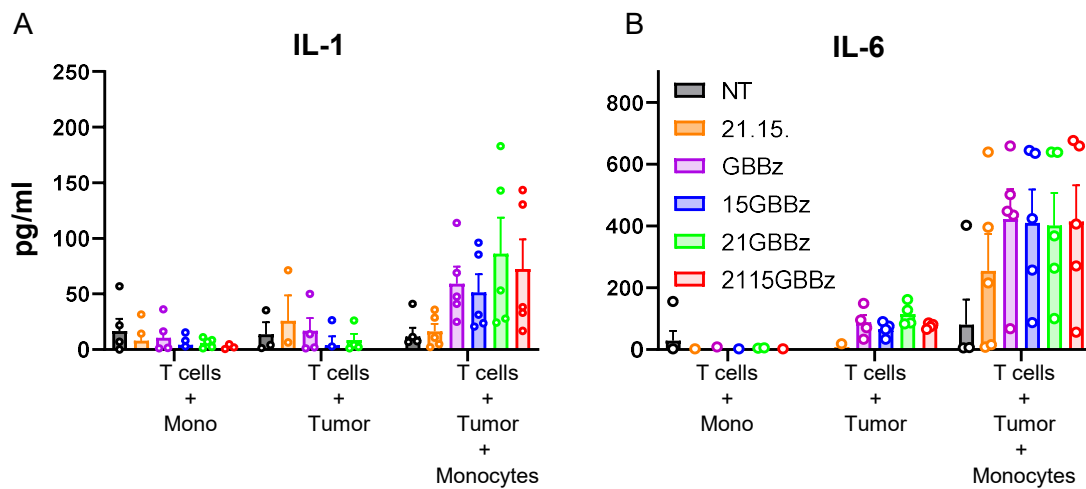
Supplementary Figure 1. GPC3-CAR T cells co-expressing IL-21 and/or IL-15 do not undergo autonomous growth. PBMCs were stimulated with plate bound anti-CD3/anti-CD28 antibodies and transduced. 0.5×10^6 generated CAR T cells were cultured in the absence of exogenous cytokines and were split every 2-4 days as needed to maintain optimal culture conditions. CAR T cell viability was assessed three times a week and cell survival in number of days post-stimulation is shown (Mean, \pm SD, three independent expansions evaluating three donors).

Supp Fig. 2



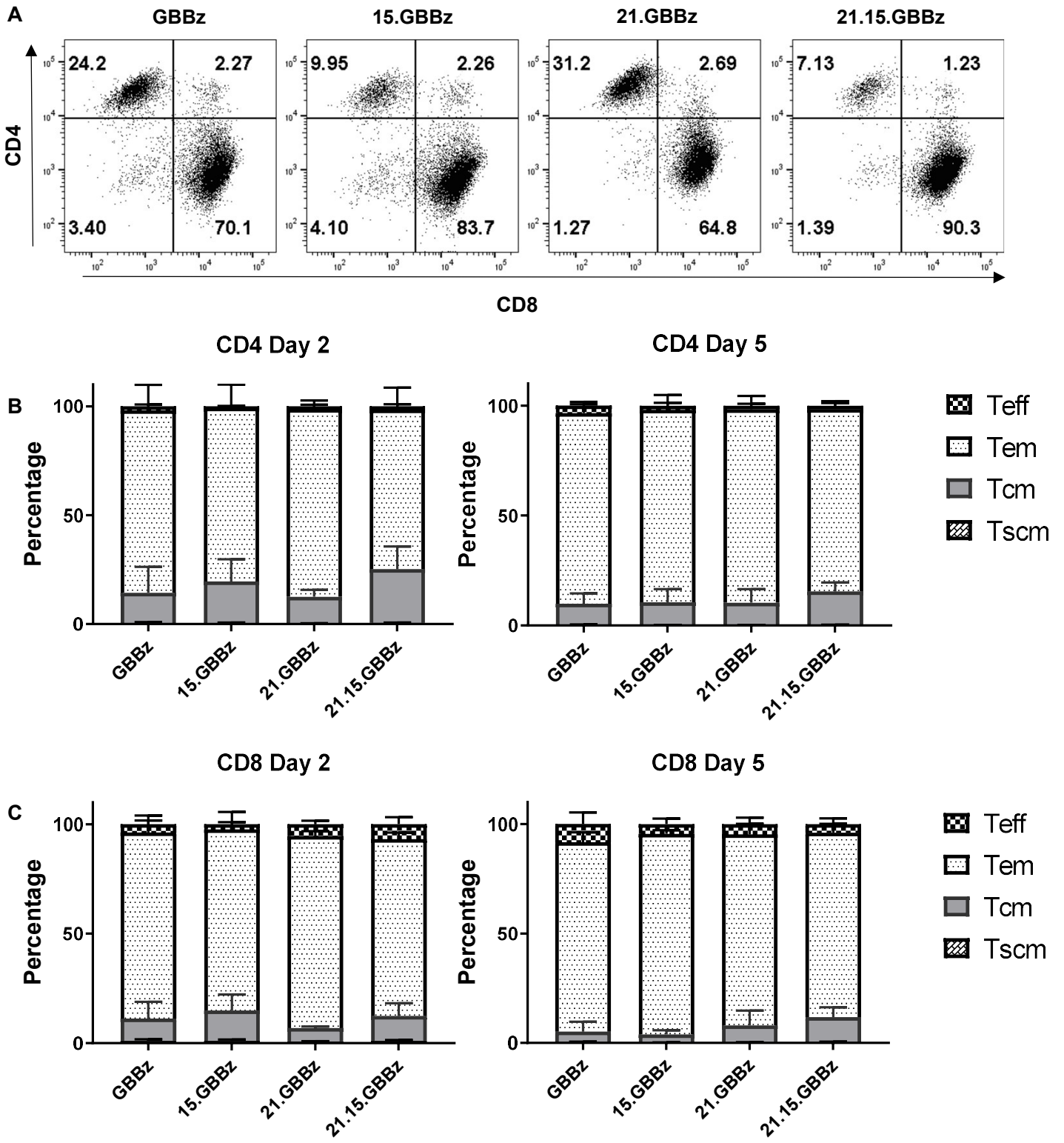
Supplementary Figure 2. CAR T cells only produce effector cytokines upon stimulation with GPC3-positive HCC cells. Production of effector cytokines **A)** GM-CSF, **B)** IL-13, **C)** IFN- γ , **D)** IL-2, and **E)** TNF- α as measured by Luminex following stimulation with either GPC3-negative A549 or GPC3-positive Huh-7 cells. (mean \pm SD; Combined data from three independent experiments evaluating six donors (Huh-7) and four experiments of four donors (A549)). Two sample t-test. Asterisks indicate significant differences for each CAR T cell group between A549 and Huh-7 co-culture conditions; ** $p < 0.01$, *** $p < 0.001$.

Supp Fig. 3



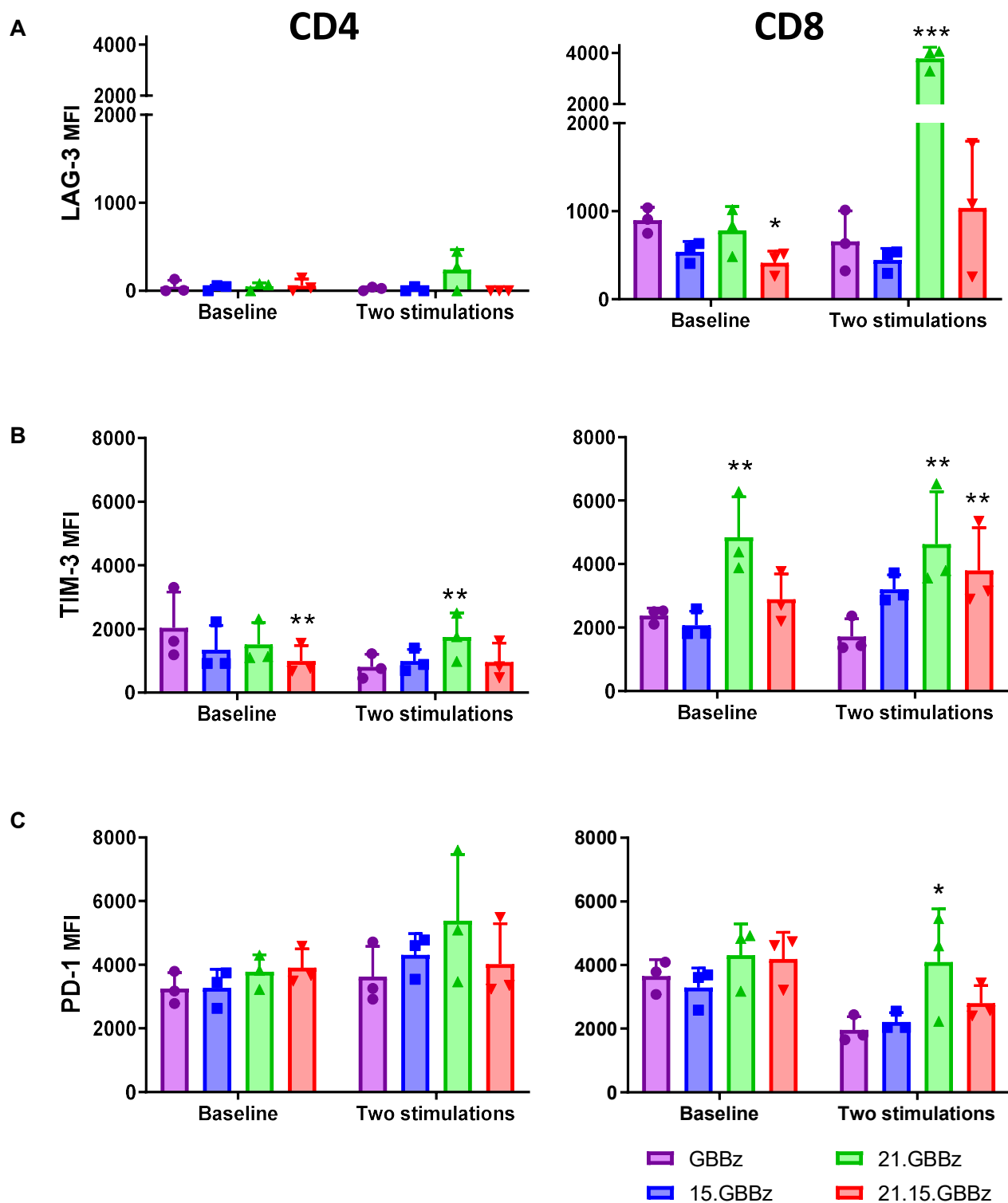
Supplementary Figure 3. Induction of IL-1b and IL-6 production in macrophages by GPC3-CAR T cells. Monocytes were negatively selected from human PBMCs from healthy donors and co-cultured with T cells expressing the indicated constructs with and without GPC3-positive tumor cells. Tissue culture supernatant was assessed at 48hrs for cytokine levels by ELISA. **A)** Levels of IL-1 increased in the presence of monocytes, tumor cells and CAR T cells compared to either tumor or monocyte plus CAR T cells. The IL-1b levels were similar in all four GPC3-CAR T cell groups. **B)** Levels of IL-6 also increased in the presence of monocytes, tumor cells and CAR T cells and the IL-6 levels were similar in all four GPC3-CAR T cell groups. Mean \pm SEM, three independent coculture experiments evaluating five donors.

Supp Fig. 4

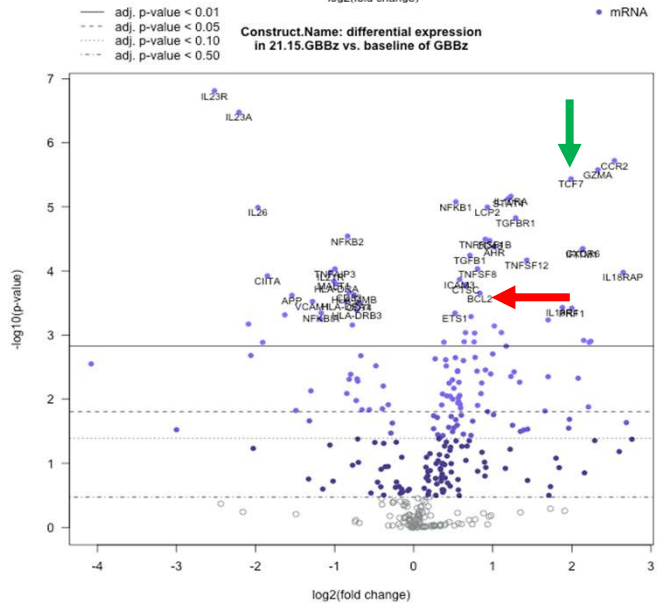
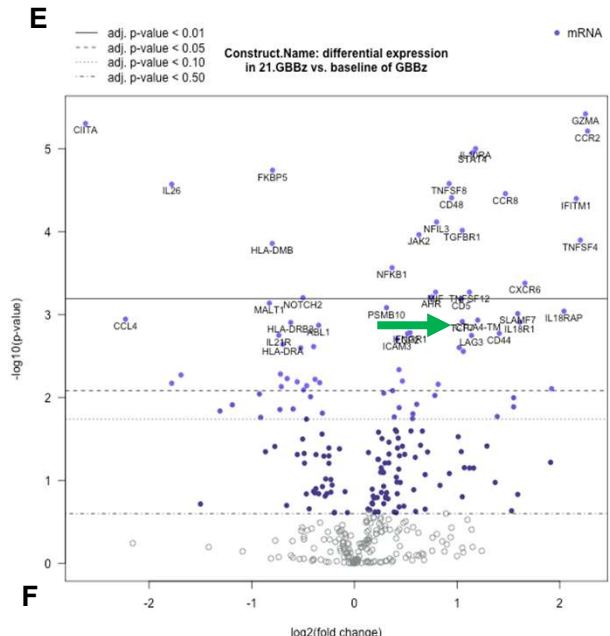
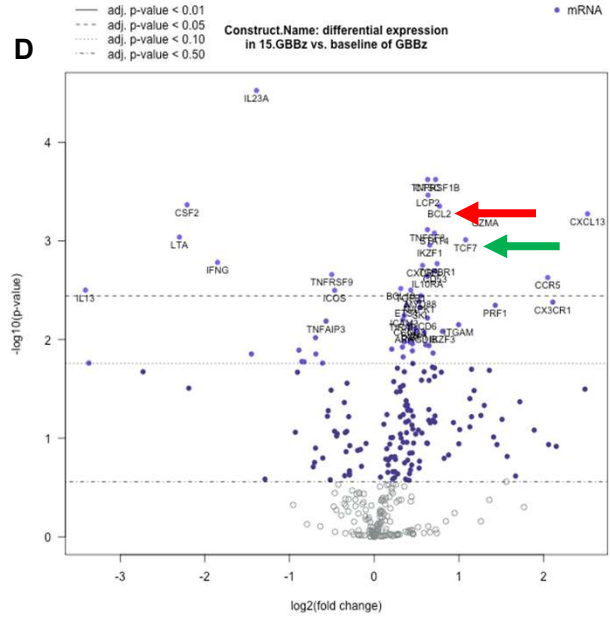
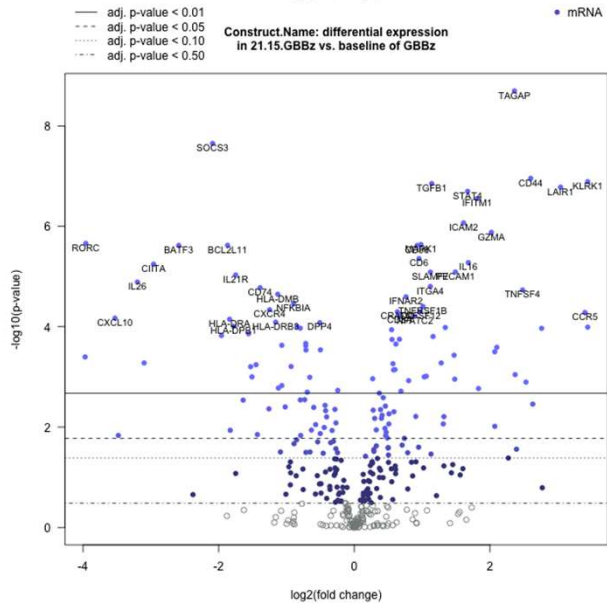
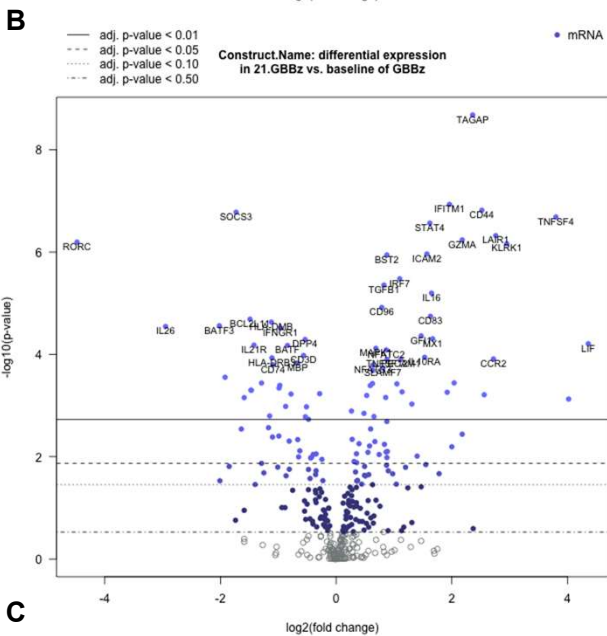
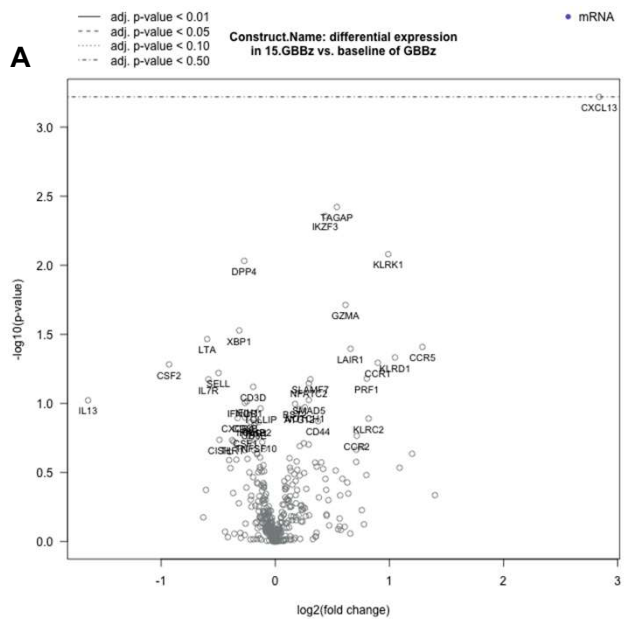


Supplementary Figure 4. Co-expression of IL-15 alone or with IL-21 increases CD8+ population but does not influence T cell memory subset composition of GPC3-CAR T cells after tumor cell killing. A) Representative dot plot showing expression of CD4 and CD8 by GPC3-CAR T cells after two consecutive stimulations with Huh-7 cells. **B-C)** Phenotype of GPC3-CAR T cells as measured by surface expression of CD45RO and CD62L in (B) CD4 and (C) CD8 GPC3-CAR T cell subsets following one (day 2) or two (day 5) stimulations with Huh-7 cells (mean \pm SEM, combined data from four independent experiments evaluating four donors). T_{scm}/T_n : CD45RO⁻/CD62L⁺, T_{cm} : CD45RO⁺/CD62L⁺, T_{em} : CD45RO⁺/CD62L⁻, T_{eff} : CD45RO⁻/CD62L⁻. One-way ANOVA.

Supp. Fig 5.

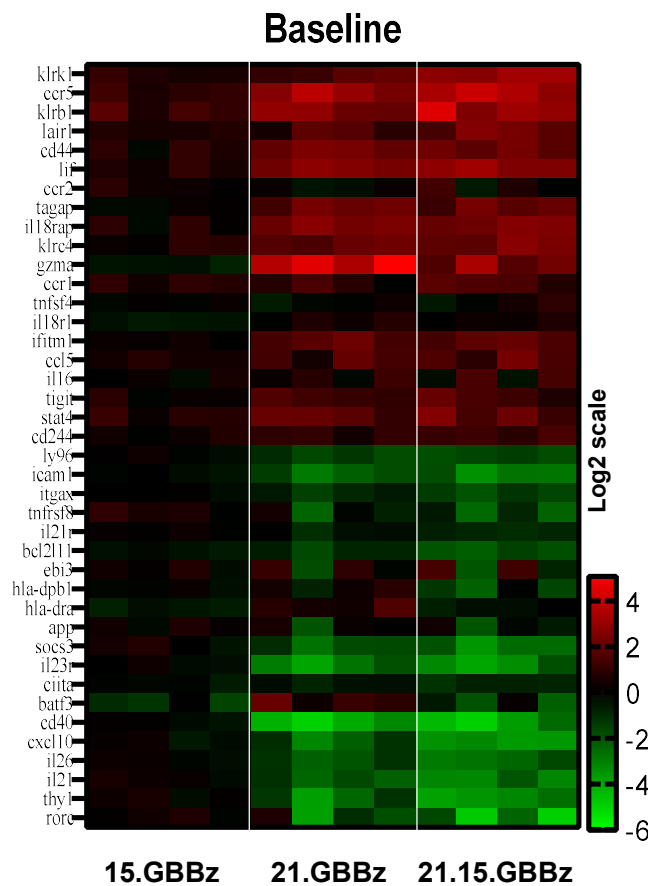


Supplementary Figure 5. Exhaustion marker expression in GPC3-CAR T cells before and after stimulation. Surface expression of (A) LAG-3, (B) TIM-3, and (C) PD-1 were assessed by flow cytometry post-manufacture (baseline) and after two stimulations with tumor cells (MFI \pm SD, combined data from three independent experiments evaluating three donors). Only MFI changes >2 fold were considered. Two-way ANOVA. * $p < 0.05$, ** $p < 0.01$, *** $p < 0.001$ (asterisks represent comparison to GBBz T cell group).

Supp Fig. 6**Baseline****Post-stimulation**

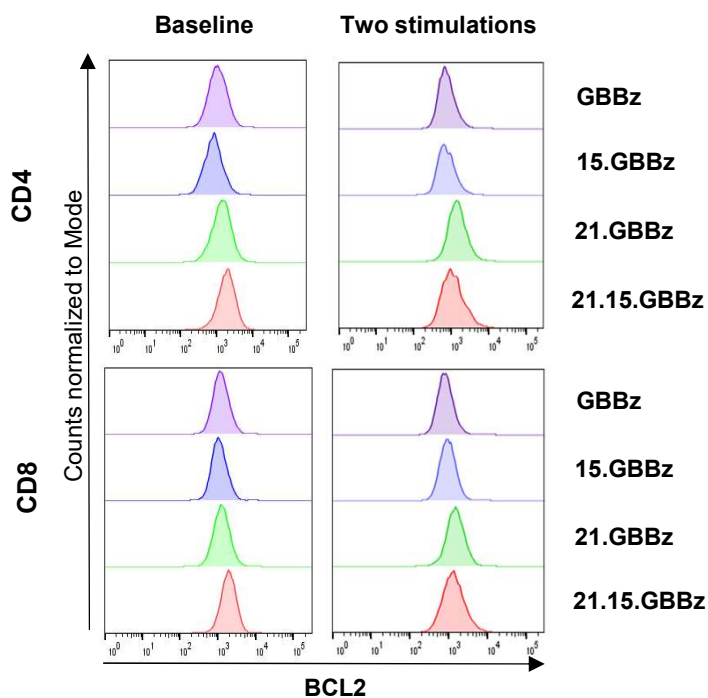
Supplementary Figure 6 GPC3-CAR T cell gene expression profiles before and after stimulation with HCC cells. Volcano plots showing \log_2 fold changes in expression for genes post-manufacture (baseline, **A-C**) or after tumor cell killing with Huh-7 cells (post-stimulation, day 3, **D-F**) using the Nanostring™ immuno-oncology panel. Panels show comparisons of gene expression in 15.GBBz (**A, D**), 21.GBBz (**B, E**), and 21.15.GBBz (**C, F**) compared to GBBz. Adjusted p-values are represented by lines across volcano plots. Green arrow: TCF7; red arrow: BCL2. Four independent cocultures evaluating four independent donors, Nanostrings performed as a single batch.

Supp Fig. 7.



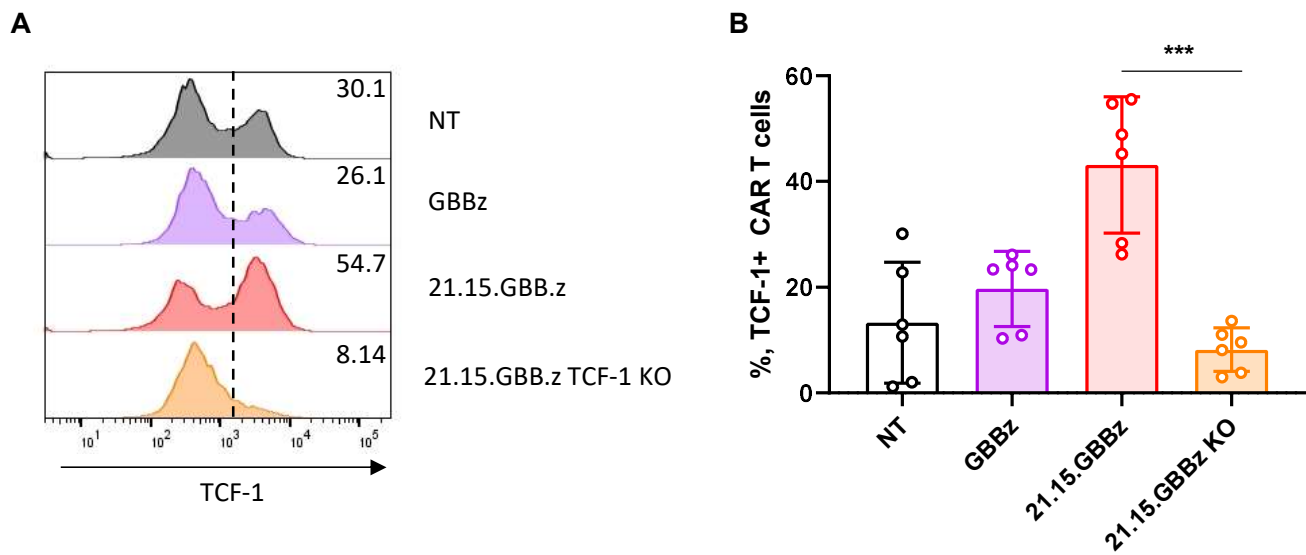
Supplementary Figure 7. GPC3-CAR T cell expression at baseline. Heat map showing fold expression changes for top 20 genes with most increase or decrease in expression and reaching significance versus GBBz T cells at baseline (arranged with respect to 21.15.GBBz vs GBBz). Multiple comparisons were performed after using Benjamini-Hochberg correction. Four independent cocultures evaluating four independent donors, Nanostrings performed as a single batch.

Supp Fig. 8.



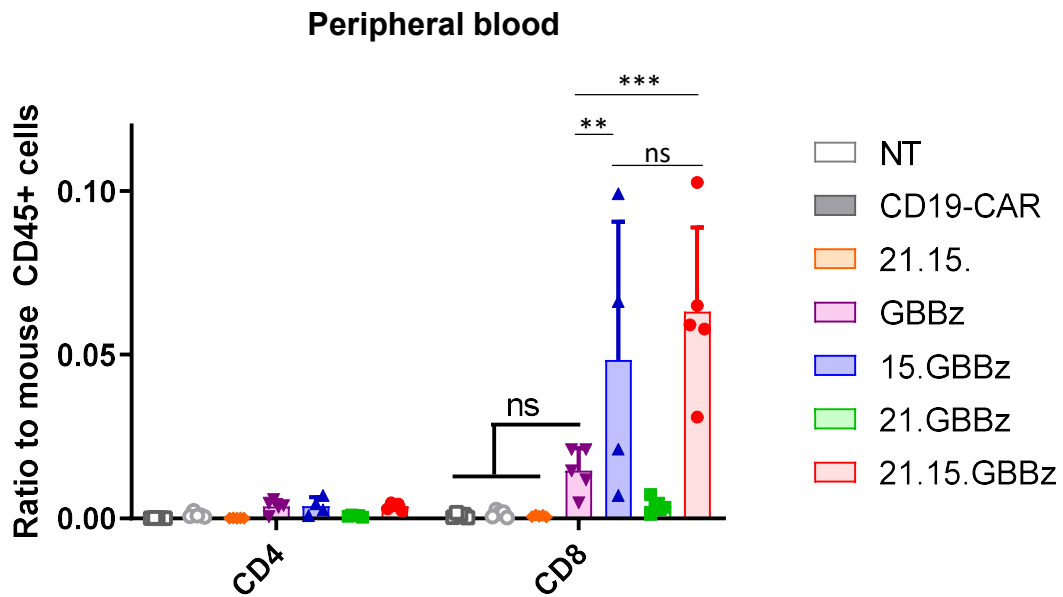
Supplementary Figure 8: BCL-2 expression in GPC3-CAR T cells: BCL-2 protein expression within CD4 and CD8 subsets of GPC3-CAR T cells was measured by intracellular flow cytometry. Representative histograms are shown for two independent measurements of indicated constructs.

Supp Fig. 8



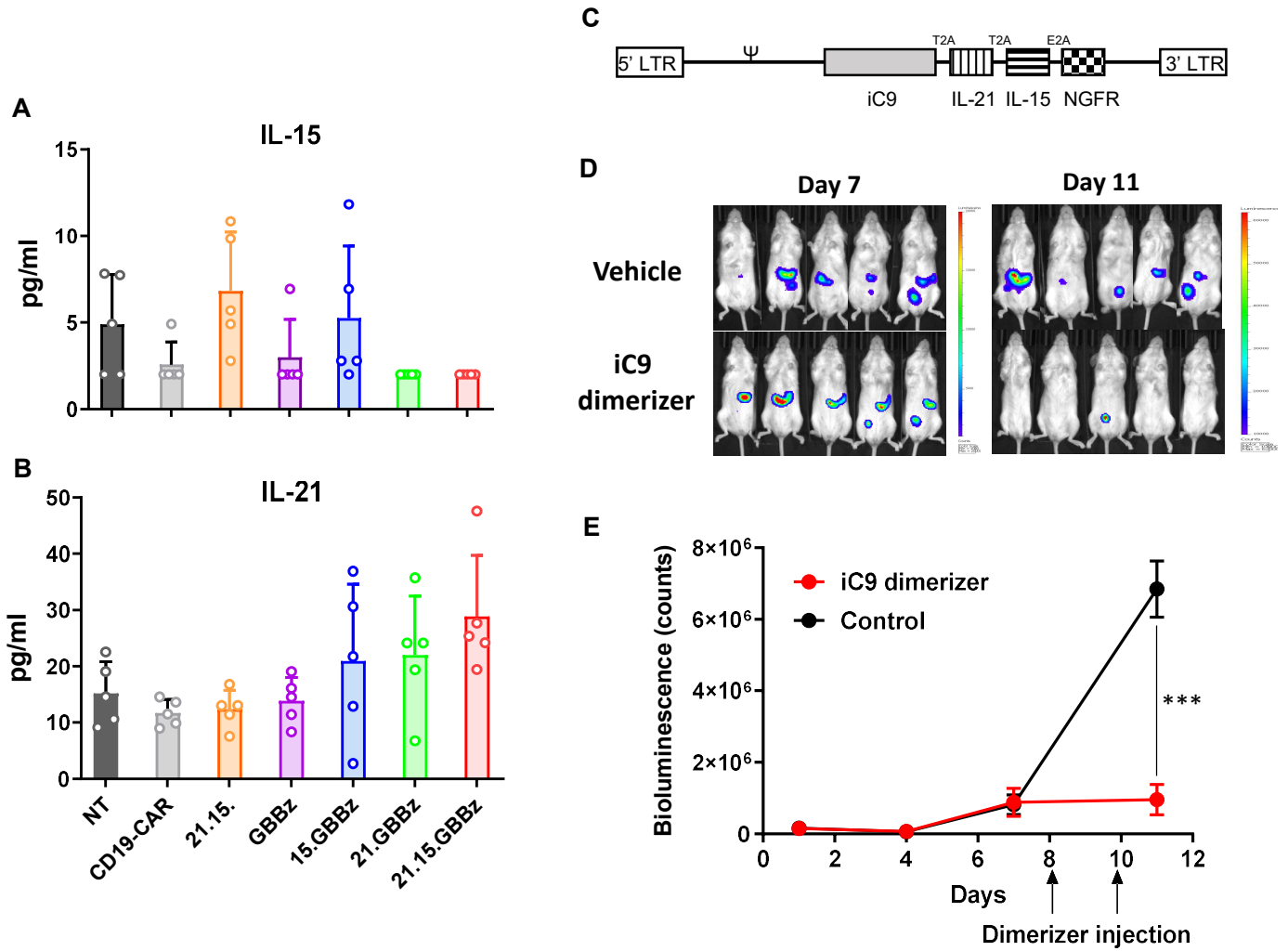
Supplementary Figure 9 Efficiency of *TCF7* knock out: After CRISPR/Cas9 mediated *TCF7* knock out, intracellular TCF-1 expression was measured by FACS. **A)** Representative histogram showing TCF-1 expression of indicated constructs of one donor. **B)** Combined results from six donors from three independent expansions (mean \pm SD, student's T-test, *** $<$ 0.001).

Supp. Fig 9.



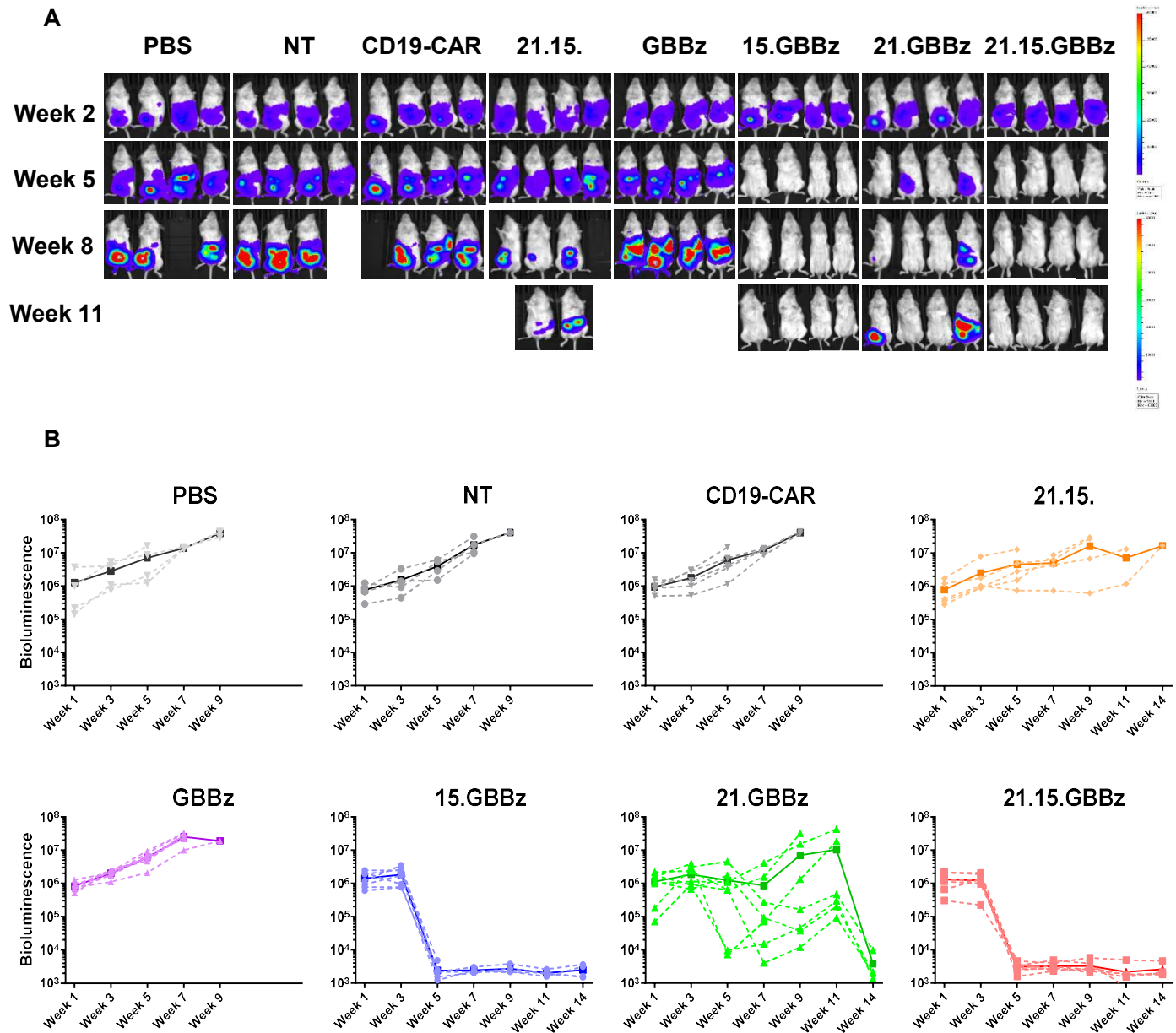
Supplementary Figure 10. GPC3-CAR T cells are detected in the peripheral blood of tumor-bearing mice 15 days after adoptive transfer. Frequencies of CD4 and CD8 GPC3-CAR T cells in the peripheral blood of treated mice were measured by flow cytometry 15 days after injection. Ratio to mouse CD45 expressing cells is shown (mean \pm SD, five mice per group). One-way ANOVA, ** $p < 0.01$, *** $p < 0.001$.

Supp Fig. 10.



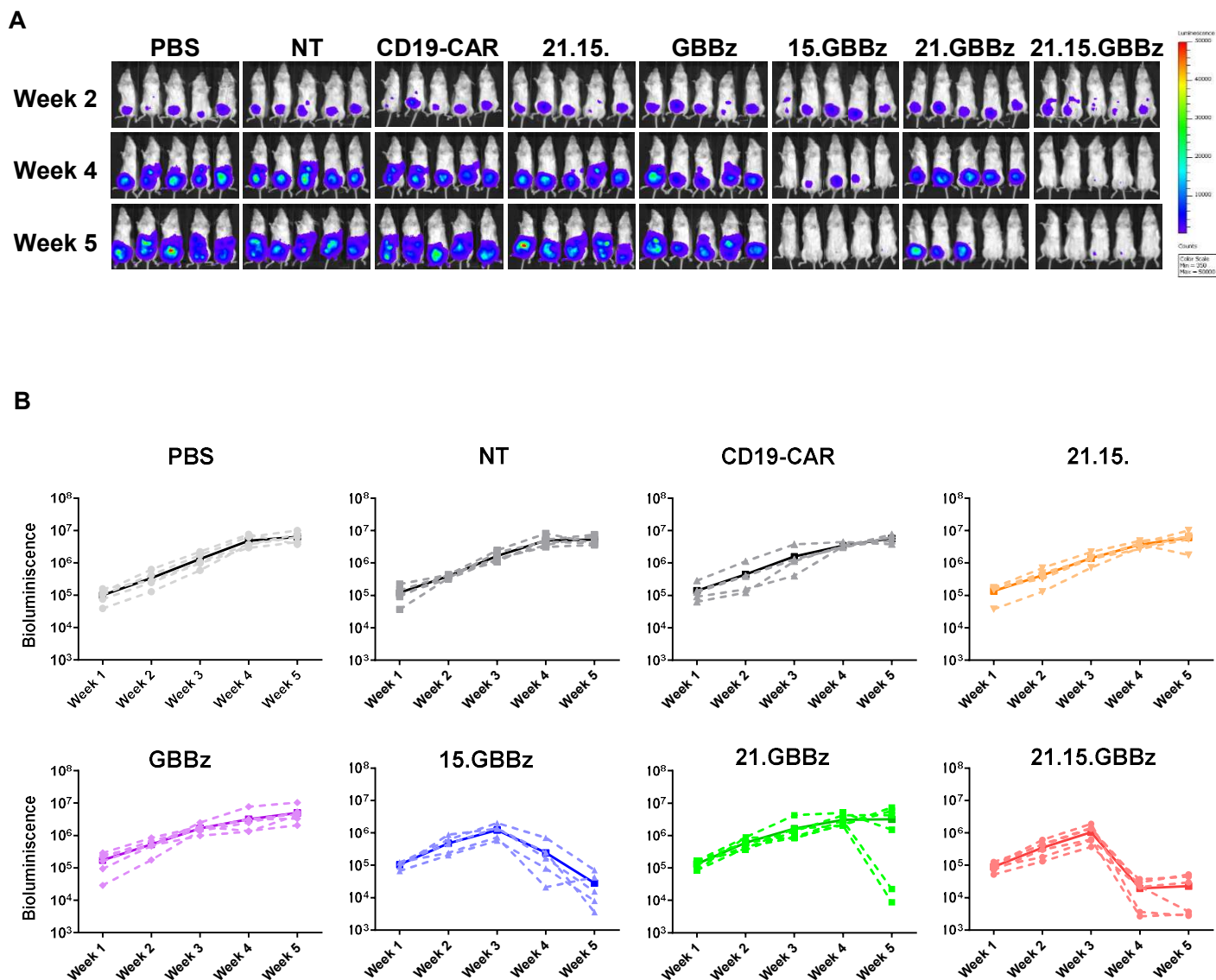
Supplementary Figure 11. In vivo safety assessment of GPC3-CAR T cells co-expressing IL-15 and/or -21. A-B) Tumor bearing mice were injected with indicated GPC3-CAR T cell groups intravenously and serum cytokine levels were measured by ELISA on Day 15 (Mean + SD, n=5). No difference was found when comparing levels with One-way ANOVA. **C)** Schematic map iC9.21.15.NGFR. This construct was used to co-transduce T cells with GBBz and Ffluc and evaluate iC9's ability to eliminate 21.15. expressing CAR T cells. **D)** Bioluminescence images at indicated timepoints before and after administration of AP20187 (iC9 dimerizer). **E)** Bioluminescence counts over time indicating the efficiency of iC9 to eliminate IL-21 and -15 expressing cells (Mean ± SD, five mice per group).

Supp. Fig 11.



Supplementary Figure 12. 15.GBBz T cells generate a comparable anti-tumor response to 21.15.GBBz in malignant rhabdoid tumor (MRT, G401) xenograft-bearing mice. NSG mice (n=4-8) were injected with 5×10^6 Ffluc+ G401 cells followed by 5×10^5 GPC3-CAR T cells on day 14. **A)** Weekly monitoring of bioluminescent G401 tumor cells. **B)** Tumor bioluminescence counts over time for each group. Dashed lines represent bioluminescence of each animal, solid lines represent mean bioluminescence for the indicated treatment group.

Supp. Fig 12.



Supplementary Figure 13. 15.GBBz T cells generate a comparable anti-tumor response to 21.15.GBBz T cells at a 2×10^6 dose in HCC xenograft-bearing mice. NSG mice ($n=5$) were injected with 2×10^6 Ffluc+ Huh-7 cells followed by 2×10^6 GPC3-CAR T cells on day 14. **A)** Weekly monitoring of bioluminescent Huh-7 tumor cells. **B)** Tumor bioluminescence counts over time for each group. Dashed lines represent bioluminescence of each animal, solid lines represent mean bioluminescence for the indicated treatment group.